Journal of Fluorescence (2019) 29:27–40
https://doi.org/10.1007/s10895-018-2305-5

ORIGINAL ARTICLE

Luminescent Sensing, Selective Extraction and Recovery of Cu^{2+} from Aqueous Environment by a Novel Turn-on Chemosensor

Soma Mukherjee [1] · Soumi Betal [1]

Received: 19 July 2018 / Accepted: 14 October 2018 / Published online: 29 October 2018

Abstract

A novel luminescent hydrazone ligand was synthesized via 1:1 condensation reaction of 9-anthracene aldehyde and 2-hydrazinobenzoic acid followed by its characterization with the help of absorption, emission, FTIR, NMR and mass studies. It was investigated as a reversible, ratiometric and turn-on luminescent chemosensor for Cu^{2+} in aqueous environment. The receptor shows a prominent color change in presence of Cu^{2+} from yellow to reddish brown in DMSO-H_2O (2:1) medium. Upon addition of Cu^{2+}, a remarkable increment in emission intensity ($\Phi = 0.091$, 11 fold) was observed probably due to intra-ligand charge transfer transition (ILCT). Interestingly, this sensor is capable to extract Cu^{2+} selectively from aqueous mixture of metal ions using dichloromethane solvent with the increased extraction efficiency from 85% (L:Cu^{2+}, 1:1) to 95% (L:Cu^{2+}, 2:1) in the pH range of 6.5–10.0. The extraction behavior of Cu^{2+} was monitored with the help of UV-Vis spectroscopy and a readily-usable smartphone to capture the RGB data which may be helpful as a field based analysis tool. In presence of Cu^{2+} (1.0×10^{-5} M), no significant interference was observed after addition of 5-fold excess of other metal ions (Zn^{2+}, Cd^{2+}, Co^{2+}, Fe^{2+}, Fe^{3+}, Ni^{2+}, Hg^{2+}, Sn^{2+}, Al^{3+}, Cr^{3+}, Mn^{2+}) in DMSO-H_2O (2:1) medium. Moreover, the ligand was regenerated (> 98%) by adjusting the pH upto 4 cycles and showed a good recyclability and reusability which might be helpful to extract Cu^{2+} efficiently from aqueous medium.

Keywords Luminescent sensor · Extraction · Recovery · Copper(II) · Hydrazone · Smart phone application

Introduction

Copper ion (Cu^{2+}) is one of the most important bio-essential metal for living organisms and plays a crucial role in many physiological processes. It is toxic (WHO >2.0 ppm) due to its accumulation in cell membranes and prevents transport across the cell wall. It causes a number of symptoms like chronic fatigue, adrenal burnout, depression, panic attack, paranoia, hallucinations, Alzheimer's, schizophrenia, etc. [1–4]. Therefore, detection, monitoring and removal of Cu^{2+} from real samples need much attention now–a-days.

It is well known that most of the fluorescent chemosensors detect Cu^{2+} by fluorescence quenching processes due to paramagnetic nature which involves charge or energy transfer mechanism [5–9]. Moreover, fluorescent sensors of Cu^{2+} with a turn-off process offer comparatively less sensitivity in presence of interfering ions (Pb^{2+}, Ni^{2+}, Hg^{2+}) due to their significant quenching effect. Therefore, synthesis of turn-on fluorescence sensors selective for Cu^{2+} received considerable attention in recent years [10–25]. But in some cases sensors with low quantum yield, less solubility, narrow pH range and irreversibility offer less potential for practical applications. Although there are a number of turn-on Cu^{2+}chemosensors but among them very few are reported as efficient extractant and recovering agent [26–41].

According to the previous literature, anthracene shows excellent photo-physical properties including high fluorescence quantum yield, chemical stability and long fluorescence lifetime which makes it appropriate for constructing a good chromo-fluorogenic sensor [11]. Till date, many anthracene based chemosensors have been designed selective for metal ions such as Hg^{2+}, Zn^{2+}, Pb^{2+}, Al^{3+}, etc. which undergo multiple step synthesis or follow complex synthetic pathway [11–13]. Moreover hydrazones (-C=N-N-) have diverse environmental and biological applications as reported earlier

Electronic supplementary material The online version of this article (https://doi.org/10.1007/s10895-018-2305-5) contains supplementary material, which is available to authorized users.

✉ Soma Mukherjee
somam580@gmail.com

[1] Department of Environmental Science, University of Kalyani, Nadia, Kalyani, West Bengal 741235, India

[14–17]. Considering the novelty of anthracene and hydrazone moieties a small molecule of anthracene-9-carboxaldehyde-benzoicacid hydrazone, L was synthesized in one-step which can detect Cu^{2+} in the real sample through turn-on sensing mechanism.

Presently, very few sensors are known which can simultaneously detect, extract or recover Cu^{2+} from real samples [26–28]. Also, significant number of efficient Cu^{2+} extractants [29–41] have been reported, but none of them are chromo-fluorogenic in nature (Table S1). Till date several advanced solvent extraction techniques have been reported for removal of metal ions in recent years [42–47] viz. solid phase extraction (SPE) and dispersive liquid-liquid microextraction (DLLME), solidified floating organic drop microextraction (SFODME), single drop microextraction (SDME), solid phase microextraction (SPME), ferro fluid based microextraction, supramolecular based liquid phase microextraction, vortex assisted liquid liquid microextraction, hollow fiber liquid-phase microextraction (HF-LPME), cloud point extraction (CPE) and classical liquid-liquid extraction (LLE) methods. Inspite of several advantages these methods also have some disadvantages such as complex determination procedure, multiple step for pre-concentration of analyte, excess time for SPE and DLLME microextraction, restricted use of solvents having melting point near room temperature for SFODME, monitoring of the rate of stirring for dislodgement of the drop in SPME, memory problem during reuse of membrane in HF-LPME [42, 45–48]. Therefore, among various methods, classical liquid-liquid extraction (LLE) technique is largely used due to its simplicity, wide applicability and low cost. Moreover, it will be more economic if a single sensor might be used for simultaneous detection, extraction and recovery.

Herein, special emphasis has been given to design and synthesize a novel, low-cost, small molecule, turn-on chromo-fluorogenic sensor L (anthracene-9-carboxaldehyde-benzoicacidhydrazone) selective for Cu^{2+} which is capable of simultaneous detection, extraction and recovery of Cu^{2+} from aqueous medium. To increase the versatility of the sensor the smart phone application and logic gate behavior have also been studied.

Experimental

Materials and Methods

All reagents, solvents and metal salts are obtained commercially from Sigma–Aldrich, Merck, SRL chemical companies and were used without further purification unless otherwise stated. In case of spectroscopic measurements HPLC grade solvents are used. Sartorius CP64 balance was used for weighing purpose. ^{1}H NMR in DMSO-d_6 were recorded in Bruker 400 with trimethylsilane (TMS) as internal standard at 298 K. FTIR data were collected with the help of Shimadzu FTIR 8400. UV-Vis spectra were measured from Shimadzu UV-1700 spectrophotometer and corrected for background due to solvent absorption. Emission spectra were recorded in the Hitachi F-7000 spectrofluorimeter equipped with quartz cuvettes of 1 cm path length containing a xenon lamp as the excitation source. Mass spectra were recorded using Xevo G2-SQT.

Synthesis

The ligand (L; anthracene-9-carboxaldehyde-benzoicacidhydrazone) was synthesized by dropwise addition of a methanolic solution (7 ml) of 9-anthracenealdehyde (0.041 g. 0.2 mmol) to a methanolic solution (7 ml) of 2-hydrazinobenzoic acid hydrochloride (0.038 g. 0.2 mmol) with stirring for 30 min at room temperature (25 °C). The bright yellow color solution was filtered and the solvent was evaporated by rotary evaporator to obtain a bright yellow compound. Yield: 92%. ^{1}H NMR (400 MHz, DMSO-d_6): δ ppm 11.628 (s, 1H), 9.321 (s, 1H), 8.797 (m, 1H), 8.775 (m, 1H), 8.639 (s, 1H), 8.141–7.542 (m, 9H), 6.871 (m, 1H), 6.853 (m, 1H) [Fig. S1]. ^{13}C NMR (400 MHz, DMSO-d_6): δ ppm 169.87, 147.45, 139.68, 135.16, 131.85, 131.48, 129.79, 129.29, 128.78, 127.17, 126.79, 125.92, 125.62, 118.41, 113.40, 110.66 [Fig. S2]. FTIR (KBr pellets, cm^{-1}): 3356, 3065, 2921, 2899, 1950, 1734, 1699, 1661, 1597, 1463, 1350, 1319, 1306, 1285, 1205, 1170, 1156, 1113, 1094, 1060, 1037, 965, 933, 817, 809, 788, 737, 708, 693, 632, 622, 573, 496 [Fig. S3]. UV-Vis (DMSO/H_2O, 2:1; pH, 7.0): λ_{max} (nm) (ε, M^{-1} cm^{-1}): 320 (22,100), 418 (33,000). Mass: m/z (ESI) [M] 340.12 (calculated 340.37) (Scheme 1) $[M+H]^+$ 341.12 (calculated 341.38) [Fig. S4]. Emission: λ_{ex}, 380 nm (isosbestic) and λ_{em}, 455 nm. Quantum yield (φ): 0.008.

Spectroscopic Studies

It is well established that a sensor must effectively signal ionic metal targets and work in aqueous environment for practical application. UV-Vis and fluorescence experiments were performed using a stock solution of L (1.0×10^{-3} M) in DMSO/H_2O (2:1). Metal ions (as chloride salts, 1.0×10^{-3} M in DMSO/H_2O (2:1)) were added to the solution (DMSO/H_2O) of L and used for UV-Vis and fluorescence titrations, competitive experiments and Job's Plot. Spectroscopic studies were carried out in 10-mm quartz cuvettes at 25 °C. Every titration was repeated at least thrice until consistent values were obtained. The selectivity of L for Cu^{2+} over other metal ions was investigated both spectrofluorimetrically and spectrophoto-metrically. The binding stoichiometry for complexation reaction was ascertained by Job's continuous variation method

Scheme 1 Synthesis of L

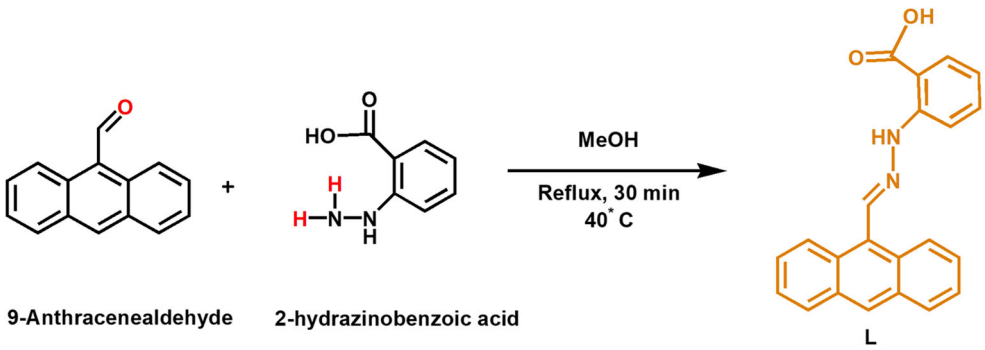

[37–40] [Fig. S5]. The association constant (K_{ass}) of the L-Cu^{2+} complex was estimated from the fluorescence titration in DMSO/H_2O (2:1) by a nonlinear least squares fitting of the data according to Eq. 1.

$$X = X_0 + (X_{lim}–X_0)/2C_0 \left[C_H + C_G + 1/K_{ass} – \left\{(C_H + C_G + 1/K_{ass})^2 – 4C_HC_G\right\}^{1/2}\right] \quad (1)$$

where, X represents the fluorescence intensity, X_{lim} represents fluorescence intensity at full complexation, C_0 is the initial concentration of the ligand, C_H and C_G are the corresponding concentrations of the ligand and metal ion during titration. Quantum yields (φ) were calculated in DMSO/H_2O (2:1) by standard method using Eq. 2 with respect to the quinine sulfate as standard reference compound.

$$\phi = Q_R \times (I/I_R) \times (OD_R/OD) \times \eta^2/{\eta_R}^2 \quad (2)$$

The Limit of detection was calculated spectrofluorimetrically using Eq. 3.

$$\text{Limit of detection (LOD)} = 3\sigma/k \quad (3)$$

where, σ is the standard deviation of blank measurement, k is the slope between the ratio of fluorescence intensity vs [Cu^{2+}].

Limit of quantification (LOQ) was calculated spectrofluorimetrically using Eq. 3:

$$\text{Limit of detection (LOQ)} = 10\sigma/k \quad (4)$$

where, σ is the standard deviation of blank measurement, k is the slope between the ratio of fluorescence intensity vs [Cu^{2+}].

Results and Discussion

Spectroscopic Detection of Cu^{2+}

The interaction of L with Cu^{2+} was investigated through spectrophotometric titrations, by addition of standard solution of

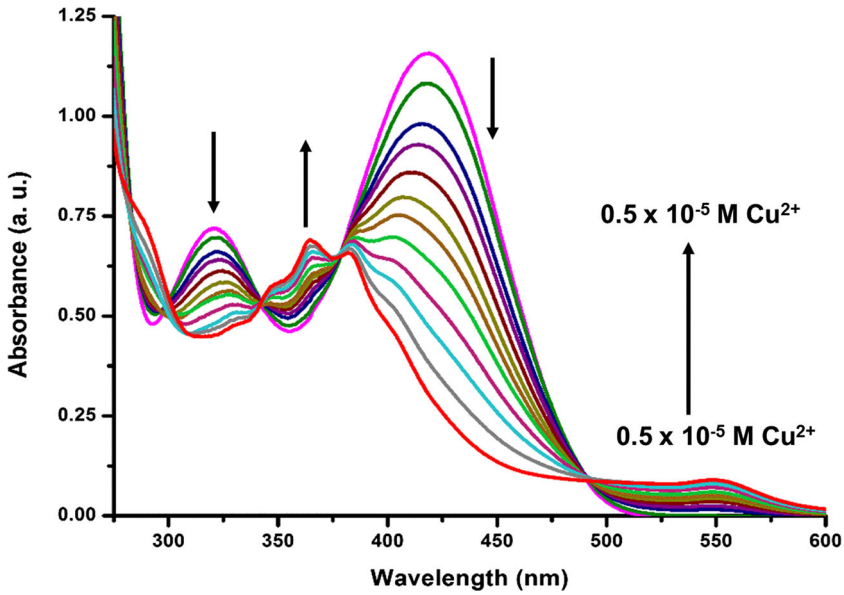

Fig. 1 Absorption spectra of L (1.0×10^{-5} M) upon addition of Cu^{2+} in DMSO /H_2O (2:1; pH = 8.0)

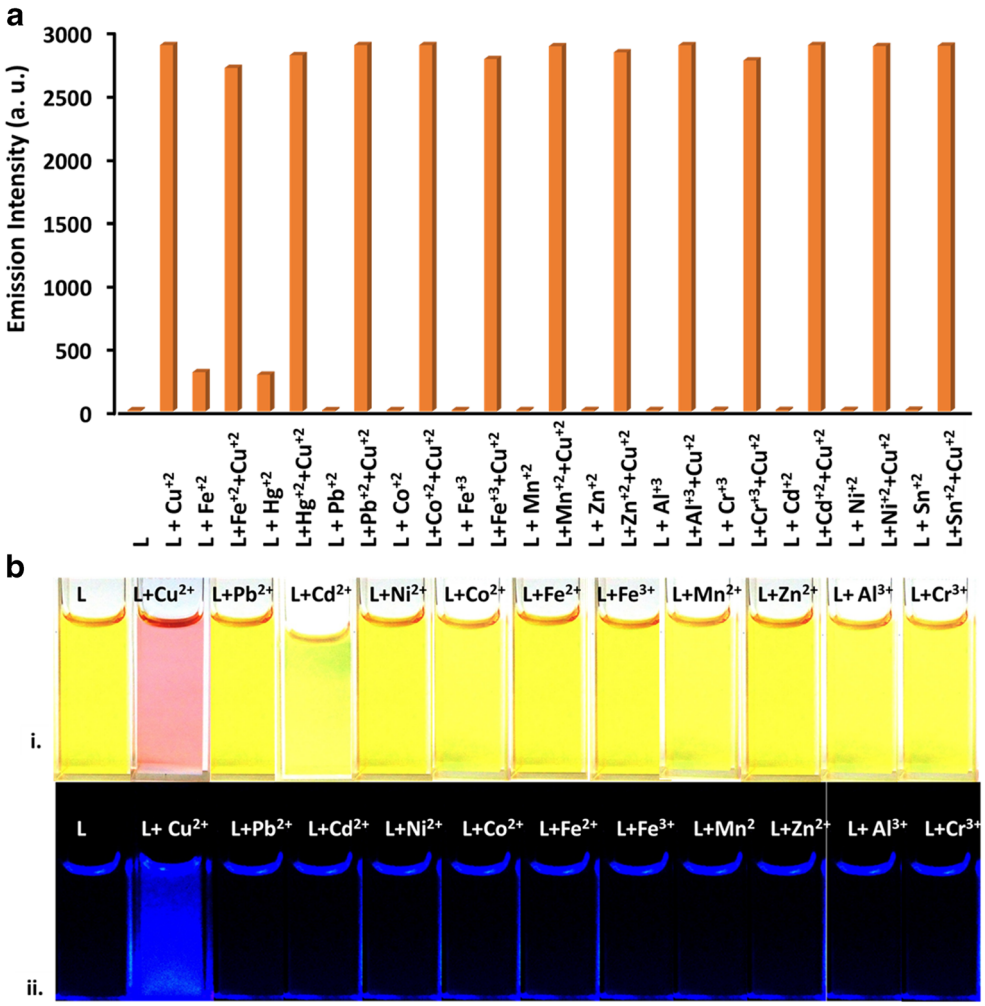

Fig. 2 **a.** The emission intensity of L (1.0×10^{-5} M) in presence of various metal ions (5 equivalents) and Cu^{2+} in DMSO/H_2O (2:1) at 298 K. **2.b.i.** Naked eye color changes of L (5.0×10^{-5} M) **2.b.ii**. Changes under UV light of L (5.0×10^{-5} M) in presence of various metal ions (5 equivalents) in DMSO/H_2O (2:1) at 298 K

Cu^{2+} in DMSO/H_2O (2:1). The receptor L exhibits the absorption peaks at 320 nm and 418 nm. Upon addition of Cu^{2+} the absorption intensity of initial peaks decreases with generation of new peaks at 365 nm and 545 nm (broad). The isosbestic points were observed at 343 nm, 380 nm and 490 nm (Fig. 1) indicating the formation of L-Cu^{2+} complex. The absorption bands in 510–575 nm region occurred may be due to metal-ligand charge transfer transition (MLCT) as reported earlier [49].

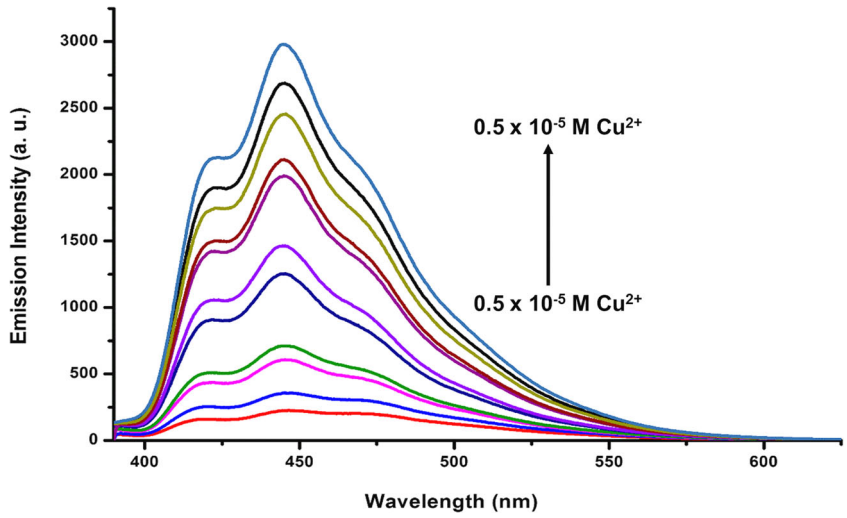

Fig. 3 Fluorescence titration (λ_{ex}, 380 nm) of L (1.0×10^{-5} M) upon addition of various amounts of Cu^{2+} ions (0.5 equivalent) in DMSO/H_2O (2:1; pH, 8.0)

Table 1 Determination of Association Constant (K_{ass}), Limit of Detection (LOD), Limit of Quantification (LOQ), Quantum Yield (Φ)

Compound.	K_{ass} (M^{-1})	LOD (M)	LOQ (M)	Φ
L	–	–		0.008
L-Cu^{2+}	$(5.14 \pm 0.005) \times 10^5$	$(5.3255 \pm 0.06) \times 10^{-10}$	$(1.7751 \pm 0.06) \times 10^{-9}$	0.091

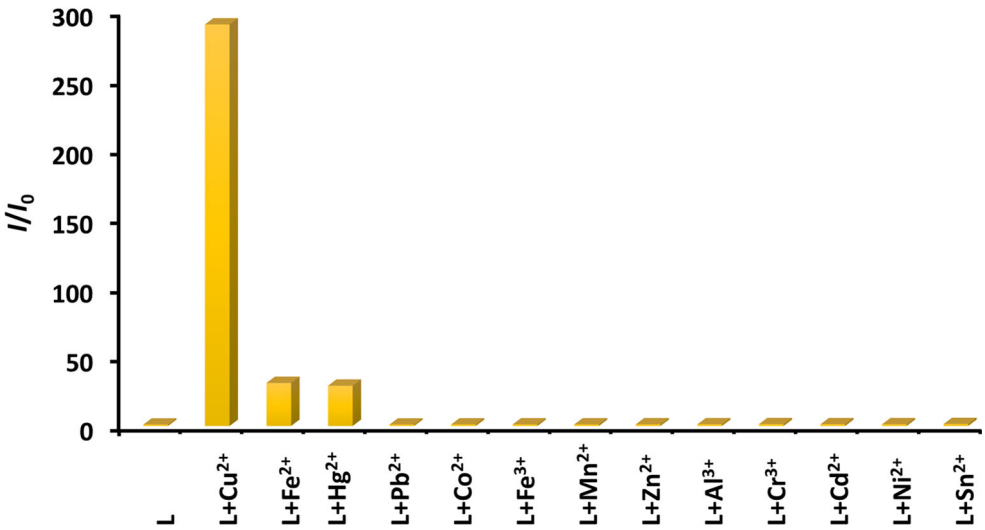

Fig. 4 Emission intensity ratios (I/I_0) for L at 455 nm in the presence of different metal ions in DMSO/H_2O (2:1; pH = 8.0) at 298 K

The Job's plot (Fig. S5) was performed to determine the binding stoichiometry between L and Cu^{2+} and was found to be 2:1 (L:Cu^{2+}). Moreover in the competitive experiment no color change of the solution in both naked eye and UV light were observed after addition of 5 equivalents of different metal ions (Zn^{2+}, Cd^{2+}, Co^{2+}, Fe^{2+}, Fe^{3+}, Ni^{2+}, Hg^{2+}, Sn^{2+}, Al^{3+}, Cr^{3+} and Mn^{2+}) to L (1.0×10^{-5} M) in DMSO/H_2O (2:1) (Fig. 2a). Upon addition of Cu^{2+} to the ligand L (DMSO/H_2O; 2:1), the color of the solution changed from yellow to reddish brown which was observed by the naked eye (Fig. 2bi) and emits in the blue region under UV light as depicted in Fig. 2bii.

Upon excitation at 380 nm the receptor L exhibits weak fluorescence (Φ, 0.008) in blue region at 455 nm in DMSO/H_2O (2:1) medium. Upon addition of Cu^{2+} upto 0.5 equivalents, a remarkable increase in emission intensity was observed at 455 nm (λ_{em}) (Fig. 3) with ~11 times increment in quantum yield (Table 1) and a value of I/I_0 ~290 (Fig. 4). The linear change of emission ratio (I/I_0) with Cu^{2+} is shown in Fig. 5. No significant spectral changes were observed after addition of 5 equivalents of other metal ions viz. Zn^{2+}, Cd^{2+}, Co^{2+}, Fe^{2+}, Fe^{3+}, Ni^{2+}, Hg^{2+}, Sn^{2+}, Al^{3+}, Cr^{3+} and Mn^{2+} (Fig. 4, Fig. S6).

The association constant (K_{ass}) of the L-Cu^{2+} complex in DMSO/H_2O (2:1) was calculated from Eq. 1 using

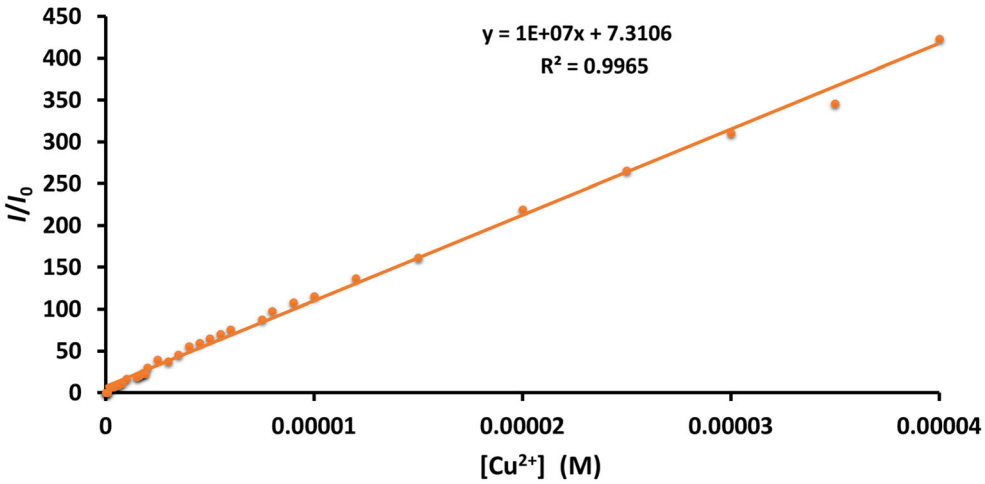

Fig. 5 The plot of emission ratio (I/I_0) vs Cu^{2+} concentration

Scheme 2 Proposed mode of sensing

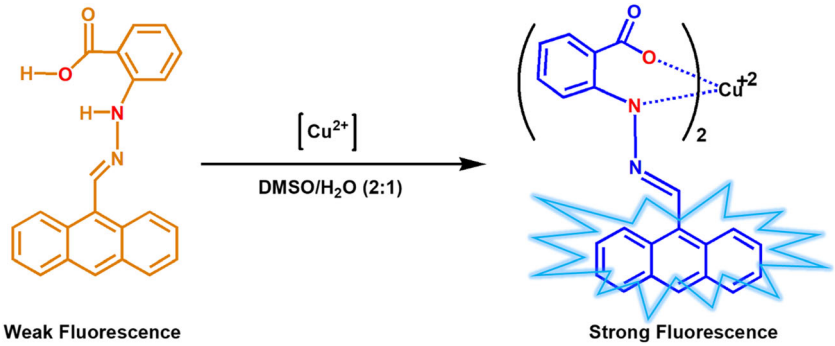

emission data. The association constant, limit of detection (LOD), limit of Quantification (LOQ) and quantum yield (Φ) are given in Table 1.

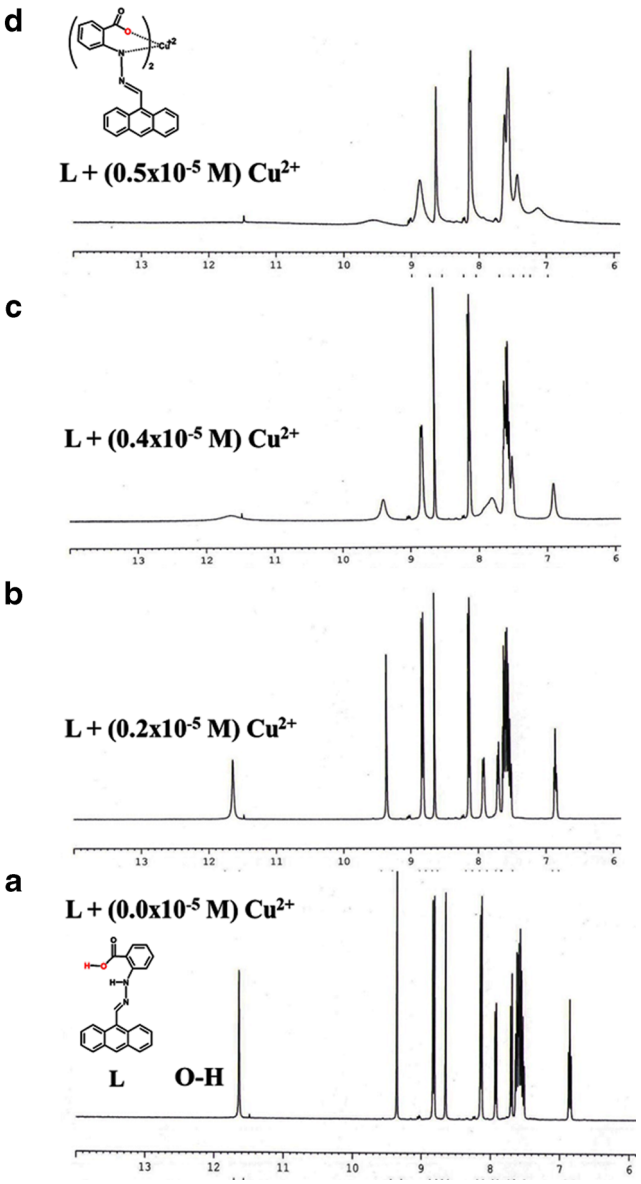

Fig. 6 Partial ^{1}H NMR (400 MHz) spectra of receptor L in DMSO-d_6 in presence of (**a**) 0.0, (**b**) 0.2, (**c**) 0.4, (**d**) 0.5 equivalents of Cu^{2+}

Sensing Mechanism

NMR Titration

In the presence of Cu^{2+} the receptor L showed a steady increment in emission intensity at 455 nm in DMSO/H_2O (2:1) medium. The H^1NMR titration studies were carried out in DMSO-d_6 and it was found that the peak intensity of –OH proton in 1.0 equivalent L gradually decreased upon addition of Cu^{2+} upto 0.5 equivalent due to the deprotonation which signifies the probable binding of 2:1 in L-Cu^{2+} (Scheme 2) Fig. 6 [11, 12, 25].

DFT and TD-DFT Calculations and Correlation with Spectroscopic Transitions

The mechanism was further explained from DFT and TDDFT studies. The highest occupied molecular orbital (HOMO) and lowest unoccupied molecular orbital (LUMO) of complex are presented in (Fig. 7). The HOMO orbital and LUMO+3 orbital of α spin and HOMO-1 orbital and LUMO+3 orbital of β spin were given in Fig. 7. Main calculated vertical transitions with compositions in terms of molecular orbital contribution of the transition, vertical excitation energies and oscillator strength are tabulated in Table 2.

The increment of turn-on phenomenon of L in DMSO in presence of Cu^{2+} is due to the intra ligand charge transfer transition (ILCT) as revealed from theoretical studies. It can be concluded from all the transitions that only ^{3}ILCT is the main reason for the emission peak observed at ~382 nm as because the electron spin density concentrated only in anthracene moiety for all the frontier molecular orbitals. The theoretical emission spectrum of L-Cu^{+2} complex is shown in Fig. S7. On excitation of absorption peak at ~ 335 nm the complex (L-Cu^{+2}) emitted at ~382 nm (λ_{theo}) which was compared with the experimental emission (λ_{exp}) value in Table 2.

Computational Details

To obtain a theoretical aspect of the structural changes of ligand upon deprotonation and coordination with Cu^{2+},

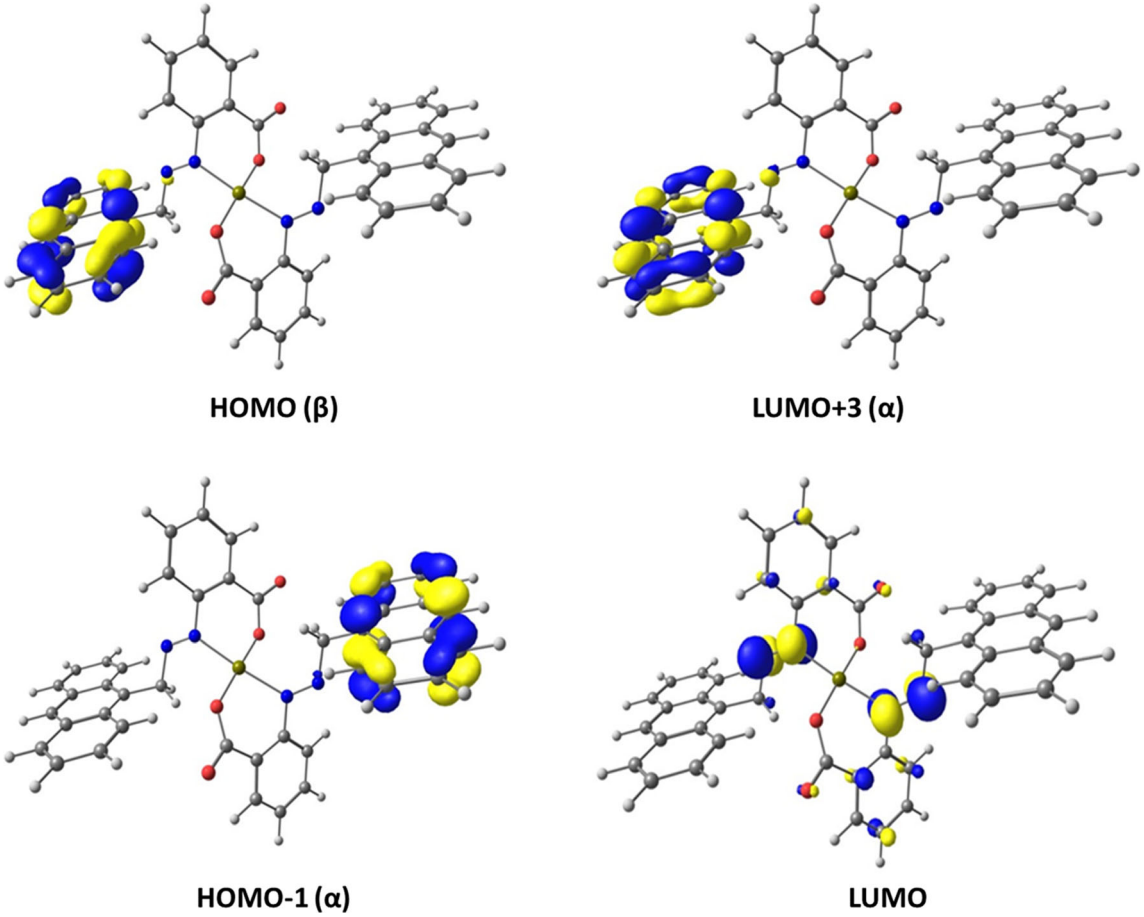

Fig. 7 Frontier orbitals involved in emission transitions

extensive density functional theory (DFT) calculations were performed. DFT optimizations of L–Cu^{2+} were carried out with the uB3LYP/6-31G^{+} for H atom and 6-31G^{+}(d,p) for C, N, O atoms method basis set using the Gaussian 09 program. For Cu^{2+}, where the LANL2DZ effective core potential (ECP) was employed. The TDDFT calculations were carried out in similar method. Ligand is designated as L.

Binding Reversibility and Logic Gate Behavior

The sensing mechanism was well supported by the reversibility of L-Cu^{2+} complex in DMSO/H_2O (2:1; pH, 8.0). Upon subsequent addition of $C_2O_4^{2-}$ the emission peak at 455 nm was completely quenched probably due to the CuC_2O_4 formation [50]. The emission intensity was restored again after addition Cu^{2+} at 445 nm. These observed changes were almost reversible even after 4 cycles with the alternative addition of Cu^{2+} and $C_2O_4^{2-}$ (Fig. 8). Thus, the receptor might be used as a reversible fluorescent sensor of Cu^{2+} in aqueous environment. Similar type reversibility was best observed by other chelators such as: EDTA, CN^{-}, PO_4^{3-} and S^{2-} but the best reversibility was observed by $C_2O_4^{2-}$ (Fig. S8). Moreover the reversible behavior of the sensor was compared with logic gate as Cu^{2+} and $C_2O_4^{2-}$ as chemical inputs and fluorescence as output (Fig. 9a).

Table 2 Calculated excited state of L-Cu^{+2} complex based on the lowest lying triplet state geometry

Composition	E (eV)	Oscillator strength (f)	CI	λ_{theo} (nm)	λ_{exp} (nm)	λssign
HOMO(α)➔LUMO+3(α)	3.2416	0.0847	0.45955	382	455	^{3}ILCT
HOMO-1(β) ➔LUMO+3(β)			0.45497			^{3}ILCT

Main calculated vertical transitions with compositions in terms of molecular orbital contribution of the transition, vertical excitation energies and oscillator strength

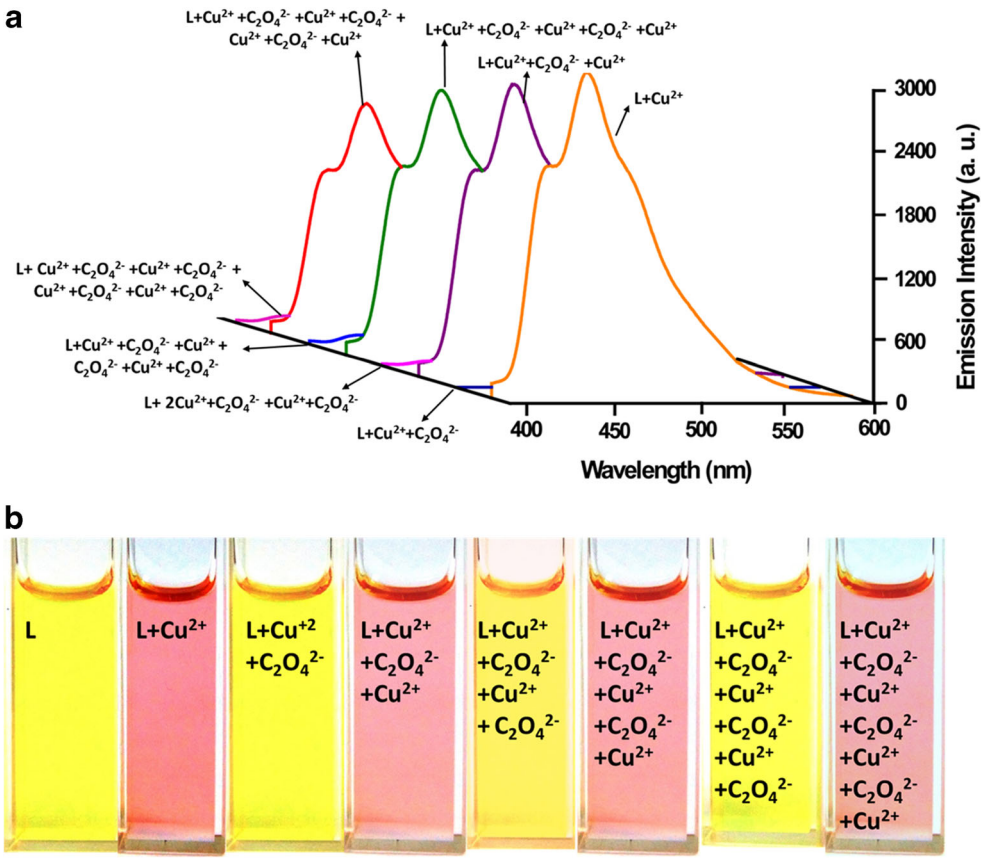

Fig. 8 Reversible changes in the emission intensity of L (1.0×10^{-5} M) at 450 nm [(λ_{ex}, 380 nm, DMSO/H_2O (2:1)] upon consecutive addition of Cu^{2+} and $C_2O_4^{2-}$ solution up to 4 cycles

The sensor L shows a very weak emission which is compared to binary '0' state and the fluorescence enhancement in presence of Cu^{2+} is compared with binary '1' state. Whereas, in presence of only $C_2O_4^{2-}$ and presence of both Cu^{2+} and $C_2O_4^{2-}$ as chemical inputs, L exhibits weak fluorescence which is compared with '0' binary state. The corresponding truth table and diagram for INHIBIT logic gate are given in Fig. 9b, c.

Extraction of Cu^{2+} by L

Detection followed by the removal of heavy metal from aqueous environment is crucial for pollution abatement. Considering various advantages of two-phase liquid-liquid extraction technique herein we have carried out batch experiments using L (anthracene-9-carboxaldehyde-benzoicacidhydrazone) as extractant in dichloromethane

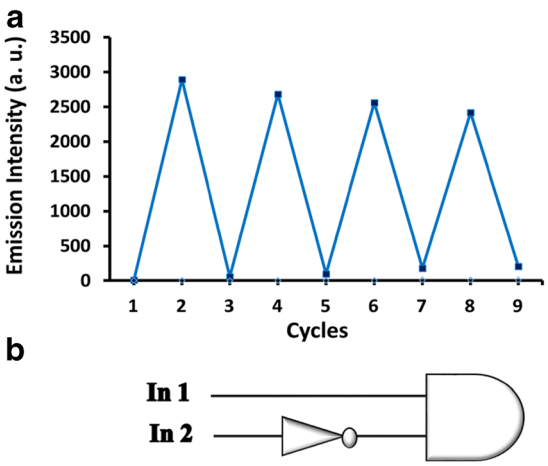

Fig. 9 Circuit diagram and truth table and for the INHIBIT logic gate

c

Truth Table

Input		Output
In 1	In 2	Out
Cu^{2+}	$C_2O_4^{2-}$	Emission at 450 nm
0	0	0
0	1	0
1	0	1
1	1	0

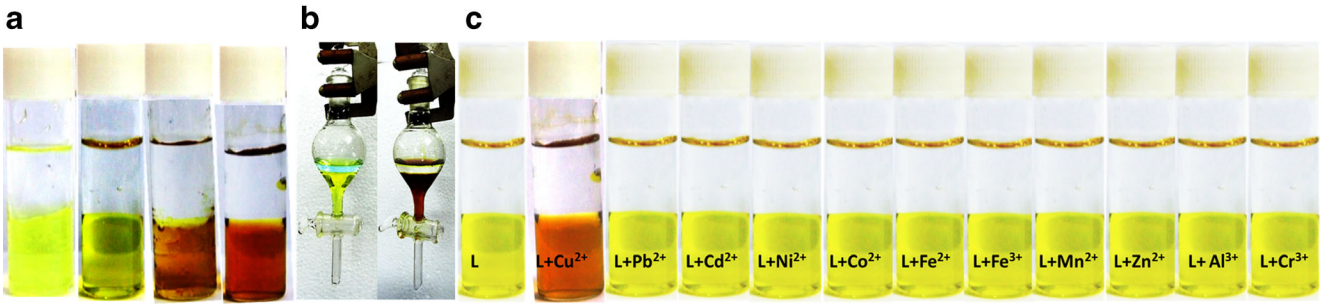

Fig. 10 **a.** Color change during extraction with varied L:Cu^{2+} ratio (1:0, 1:1, 1:2, 2:1) (pH, 8.0) in H_2O-DCM mixture (1:1). **b.** Extraction of Cu^{2+} in separation funnel. **c.** Extraction of Cu^{2+} and other metals

(DCM) and ethyl acetate with varying pH condition, shaking time, etc. to optimize the extraction condition of Cu^{2+} [50–53].

Extraction Procedure

Aqueous solutions of different metal ions (5.0×10^{-4} M) in HEPES buffer (pH 6.5–10.0) were added to equal volume of dichloromethane/ethylacetate containing the ligand L (5.0×10^{-4} M) and shaked in a mechanical shaker at 25 °C. A color change of the receptor was observed from yellow to reddish brown in dichloromethane (DCM) due to the complexation with Cu^{2+} (Fig. 10). The unknown Cu^{2+} concentration while extraction from organic phase was measured at 366 nm in UV spectrophotometer. The absorption spectra of L-Cu^{2+} (used as standard) was obtained with gradual increase of L-Cu^{2+} concentrations from 1.0×10^{-9} M to 1.0×10^{-5} M (Fig. S9) from which a calibration curve at 366 nm was plotted against varying concentrations of Cu^{2+}. The unknown Cu^{2+} concentration was estimated from this calibration curve. The diagrammatic representation of Cu^{2+} extraction is shown in Fig. 10. The Cu^{2+} concentration in aqueous phase was monitored at 604 nm using ammonium hydroxide as amine complex [54]. The unknown concentration of Cu^{2+} in aqueous phase was measured from the calibration curve of absorption intensity at 604 nm against increasing concentrations of Cu^{2+} in ammoniacal solution. The optimum pH range, shaking time and extraction mechanism were also determined.

Effect of pH on Extraction of Cu^{2+}

During the extraction of metal ions, extraction efficiencies of metal complexes are highly related to the pH of the system. Therefore, we have investigated the effective pH range of the aqueous medium by varying the pH from 3.0–11.0 using different buffer solutions. The effect of pH on absorbance of extracted L-Cu^{2+} complex were measured at λ_{max} 366 nm against reagent blank prepared in similar manner without taking Cu^{2+}. The maximum absorbance of L-Cu^{2+} complex were observed within the pH range of 6.5 to 10.0 with more than 95% extraction efficiency (Fig. 11). In acidic condition < pH 6.0, the extraction efficiency for Cu^{2+} decreased significantly probably due to the deprotonation of -NH. The pH change while complexation with Cu^{2+} is shown in Fig. S10. At pH > 11.0 the extraction efficiency decreases due to precipitation of $Cu(OH)_2$.

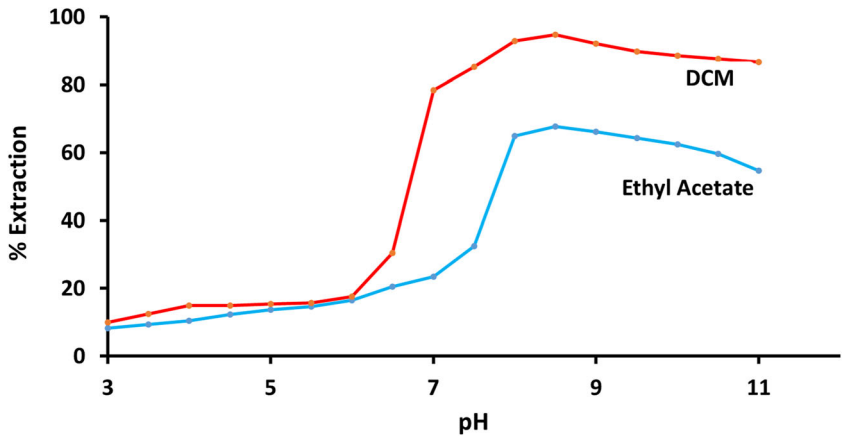

Fig. 11 Effect of pH on extraction of [L-Cu^{2+}] complex

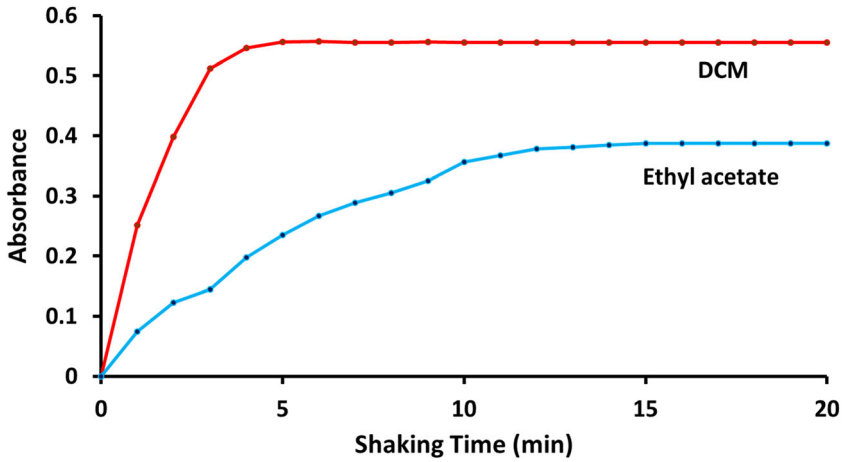

Fig. 12 Effect of shaking time on extraction of [L-Cu^{2+}]. [Cu^{2+}] = 1×10^{-4} M, L = 5 ml, 1×10^{-4} M in DCM/Ethyl Acetate; pH = 8.0 HEPES buffer; shaking time = 0–15 min; λ_{max} = 366 nm

Effect of Shaking Time

Equilibration of organic phase with aqueous phase plays a very important role in extraction procedure. Minimum extraction time is necessary for investigation of trace amounts of metal ions with high efficiency. Here, the absorbance at 366 nm was measured with varying time from 0 to 20 mins (Fig. 12). The results indicate that the optimum shaking time is 5 mins for the formation of brown red L-Cu^{2+} complex. Prolonged shaking upto 2 h has no adverse effect on the absorbance of L-Cu^{2+} complex. Hence, optimum shaking time was selected as 10 min for equilibration in subsequent experiments.

Log-Log Plot Method

In this method, amount of Cu^{2+} is kept constant and HEPES buffer of pH 8.0 is added to make up the volume up to 9 ml. The 6 ml of ligand having various concentrations (1×10^{-3}–2×10^{-2}) is added to Cu^{2+} (1×10^{-4} M) and equilibrated for 10 min. The absorbance of reddish brown colored organic phases was recorded at 545 nm against reagent blank. The composition of extracted Cu^{2+} complex is confirmed by plotting graph of Log D[Cu^{2+}] against Log C[L] (Fig. 13). The plot is linear with the slope value of 1.52 at pH 8.0, confirming

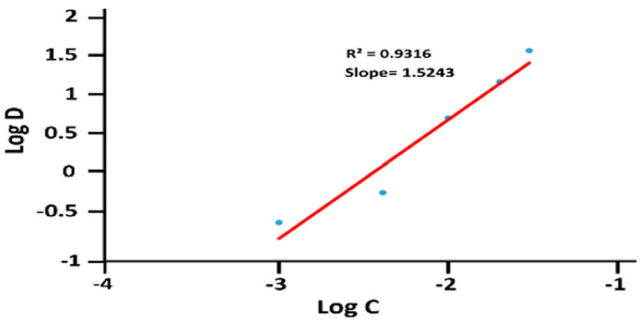

Fig. 13 LogD vs LogC plot method. Cu^{2+}, 1×10^{-3} M; L, 1×10^{-3}– 2×10^{-2} M in Dichhloromethane; pH = 8.0 HEPES buffer; shaking time = 10 min; λ_{max}, 366 nm

the composition while extraction of L:Cu^{2+}, 2:1 which was further confirmed by Job's plot [50–53].

Smart Phone Based Color Image

Images of organic phase after extraction with different concentration of Cu^{2+} was captured with RGB grabber Shunamicode application installed in a smart phone (Lenovo A 7000) and was analysed [22, 55]. At first 30 ml borosil culture tube was wrapped in carbon paper to reduce the interference of external light sources. The images of extracted organic layer containing different concentrations of Cu^{2+} [0, 0.2, 0.4, 0.6, 0.8, 1.0) $\times 10^{-6}$ M Cu^{2+}] in distilled water and were captured by RGB grabber for obtaining the values of the red (R), green (G) and blue (B) colour channel level standards (Fig. 14b). In mobile the component values are stored as integer numbers from 0 to 255. The RGB value goes up from 0 to 255 because it takes up exactly one byte of data. 1 byte is equal to 8 bits and each bit represents either a '0' or a '1' in binary system. Therefore in binary system 2^8 (=256) no. of value are obtained for each R, G, B values. Thus the values of R, G, B will vary from 0 to 255. The images were captured in the flash light taking the sample one by one in the wrapped culture tube. Next the G/R and B/R ratios were plotted to obtain the standard curves (Fig. 14a) from which the unknown concentration of Cu^{2+} in tap water and municipal waste water were determined. The absorption spectra of the same samples (L, L + Cu^{2+}) were taken which are shown in Fig. 14c [55]. The limit of detection (LOD) of the ligand for determining Cu^{2+} concentration was investigated to be 5.3255×10^{-10} M but for determination of Cu^{2+} by smart phone in real sample, Cu^{2+} was added in ppm level for better function of RGB grabber installed in smart phone (Table 3).

The concentration-dependence of the extraction data demonstrates (Fig. 10) that sensor L could colorimetrically signal Cu^{2+} in tapwater and municipal waste water upto 1.0×10^{-6} M by smart phone application. Thus the sensor L may be useful

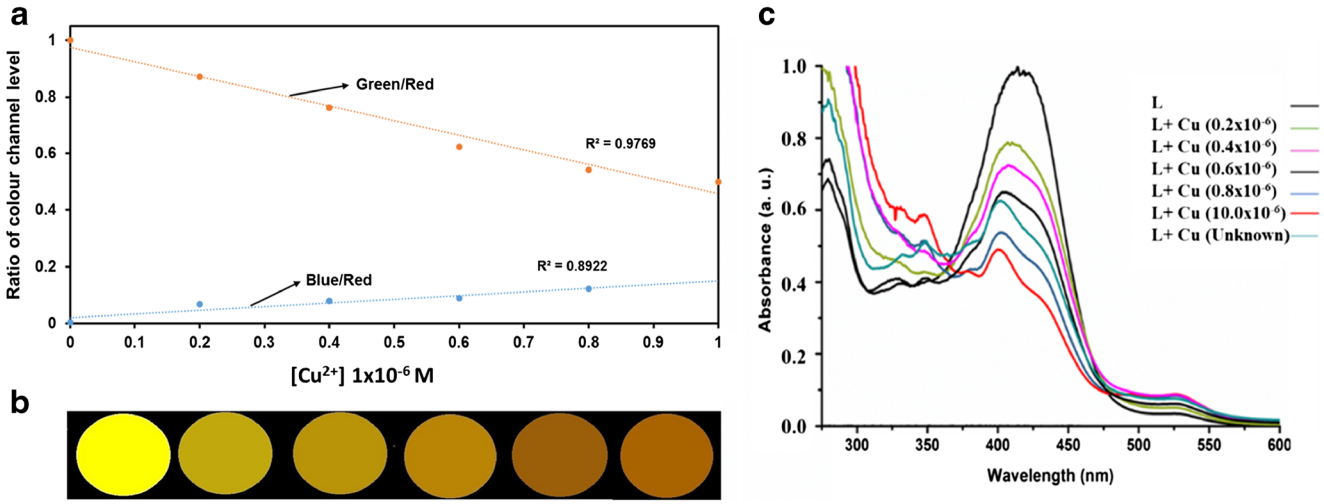

Fig. 14 **a.** Plots of the ratio of color channel level **b.** Smartphone-based image acquired using the RGB Grabber application versus $[Cu^{2+}]$ in Aqueous medium. $[L] = 1.0 \times 10^{-5}$ M in DCM, $[Cu^{2+}] = (0, 0.2, 0.4, 0.6, 0.8, 1.0) \times 10^{-6}$ M in water. **c.** UV-Vis spectra of $[L] = 1.0 \times 10^{-5}$ M in DCM, $[Cu^{2+}] = (0, 0.2, 0.4, 0.6, 0.8, 1.0) \times 10^{-6}$ M in water

Table 3 Comparison of Cu^{2+} concentration

Source	Sample Name	Initial amount of Cu^{2+} (ppm)	Amount of Add on Cu^{2+} (ppm)	Value in RGB grabber (ppm)	Value in UV Spectrocsopy Method (ppm)	Value in AAS (ppm)
Munici-pal Waste water	MW1	0.063	2.00	2.142 ± 0.007	2.071 ± 0.006	2.059 ± 0.003
	MW2	0.063	10.00	10.112 ± 0.006	10.068 ± 0.005	10.061 ± 0.004
Tap water	TW1	0.003	2.00	2.045 ± 0.007	2.050 ± 0.006	2.099 ± 0.003
	TW2	0.003	10.00	10.041 ± 0.007	10.058 ± 0.004	10.021 ± 0.004

for detection of the Cu^{2+} in real samples using a smartphone as a convenient tool (Fig. 14) in ppm level.

pH Effect on Stripping

pH plays a very important role in stripping Cu^{2+} from organic layer (dichloromethane/ethyl acetate). Herein the stripping efficiency was observed by varying the pH of the aqueous layer from 1.0–11.0 [1.0–12.0 by H_2SO_4 (pH 1.0–5.0), HEPES buffer (pH, 5.0–9.0), NaOH (9.0–12.0)] which is depicted in Fig. 15. It is seen that in pH 2.0–4.5 the stripping efficiency is maximum (~ 98%).

Stripping Isotherm Studies

In stripping isotherm the number of steps required for removal of maximum amount of Cu^{2+} from the loaded organic layer is determined. To find out the number of stages required for

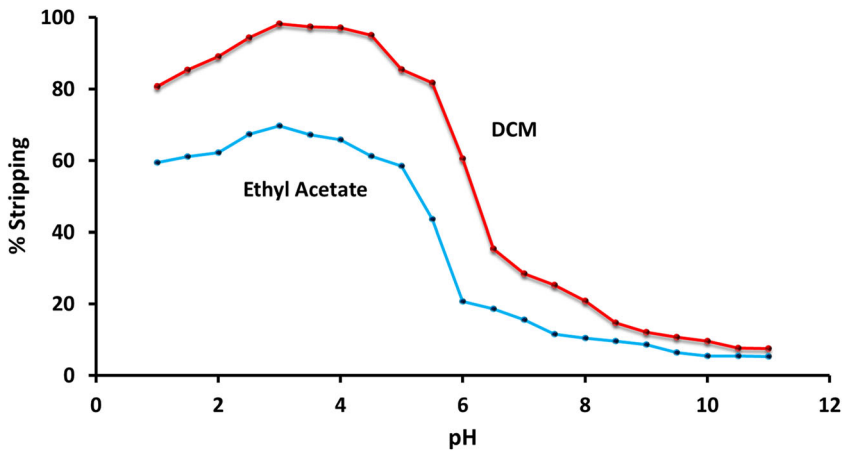

Fig. 15 Effect of pH on stripping (%) in presence of different solvents

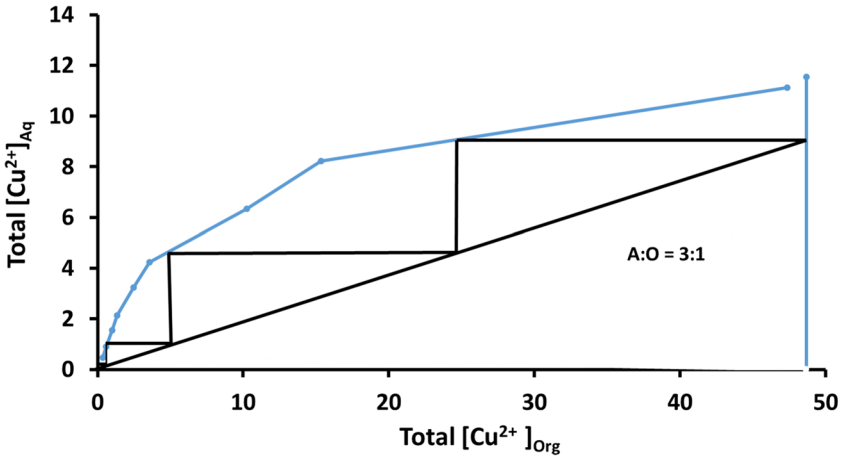

Fig. 16 Mc-Cabe Thiele diagram on stripping of total [Cu^{2+}] from loaded organic (Org) phase

stripping at chosen phase ratio, aqueous:organic (A:O), stripping isotherm plot for Cu^{2+} extraction from the loaded dichloromethane layer with acidic aqueous layer was constructed at different phase ratio in the range A:O, 5:1 to 1:5, while keeping the total volume of the phase constant [52, 53]. After phase separation, both phases were analyzed for metal concentration. As shown in the McCabe-Thiele plot (Fig. 16.), 98% of Cu^{2+} ion can be stripped of in 4 counter-current stages at A:O ratio of 3:1. 98% stripping of Cu^{2+} from loaded dichloromethane layer was achieved using 0.5 M H_2SO_4.

Applicability of the Receptor in Real Samples

The potential applicability of the ligand was examined with water sample collected from Kalyani sewage water treatment plant and surrounding tap water. At first the standard curves were plotted in RGB grabber, UV-Vis Spectroscopy and then the values were compared by RGB grabber, UV-Vis spectroscopy and atomic absorption spectroscopy (Table. 3). It is seen that the values in RGB grabber are almost near to the values of AAS values which indicates that this ligand might be used for field based detection of Cu^{2+} through smart phone. The extraction and recovery of $Cu^{2+}$is shown in Scheme 3.

Conclusion

In this work a new reversible, turn-on, luminescent chemosensor (anthracene-9-carboxaldehyde-benzoicacidhydrazone) was synthesized which showed a yellow to reddish brown color change in presence of Cu^{2+} in DMSO/H_2O (2:1) medium. The limit of detection (LOD)

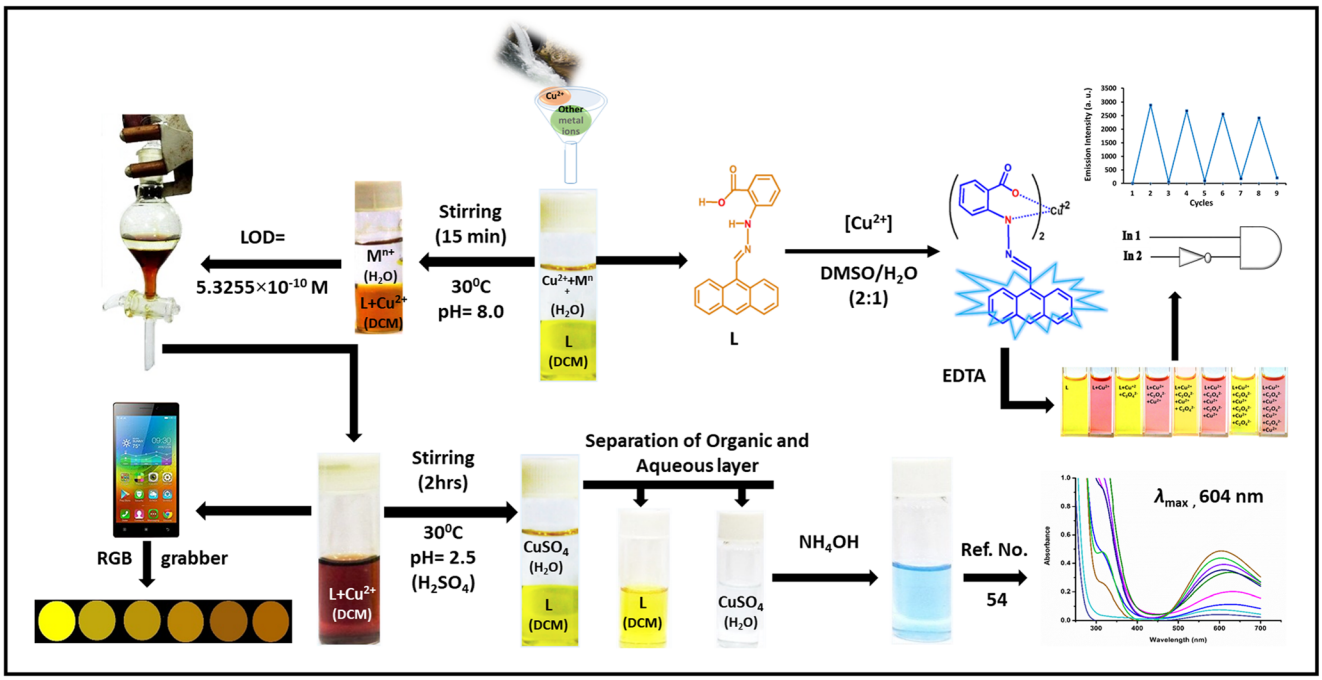

Scheme 3 Extraction and recovery of Cu^{2+}

was found in the order of ~10^{-10} M. Further it is capable of extracting Cu^{2+} selectively from aqueous mixture of environmentally significant metal ions using dichloromethane with significant efficiency. It exhibited a weak fluorescence in DMSO/H_2O medium with ~12 folds increment in emission intensity upon addition of Cu^{2+} probably due to intra ligand charge transfer transition (ILCT). The ratio of ligang/Cu^{2+} during extraction was found to be 2:1 from the slope of logD-logC plot. Almost 98% Cu^{2+} was stripped of from the mixture by adjusting the pH of aqueous medium which was revealed from McCabe-Thiele diagram. The recovered ligand showed a good recyclability and reusability for 4 cycles. Thus the receptor might be used as a low cost chromo-fluorogenic chemosensor as well as selective extracting agent for simultaneous extraction and recovery of Cu^{2+} from real samples with satisfactory efficiency and reusability.

Acknowledgments We gratefully acknowledge Women Scientist Scheme-B Internship Mode of KIRAN- Societal Research Fellowship (NASI/SoRF-I/2014-2015/68), DST, New Delhi and DST-PURSE, New Delhi for their financial support. We are also thankful to the University of Kalyani for providing infrastructural facilities.

References

1. Wasi S, Tabrez S, Ahmad M (2013) Toxicological effects of major environmental pollutants: an overview. Environ Monit Assess 185: 2585–2593
2. Khalaj M, Kamali M, Khodaparast Z, Jahanshahi A (2018) Copper-based nanomaterials for environmental decontamination – an overview on technical and toxicological aspects. Ecotoxicol Environ Saf 148:813–824
3. Egorova KS, Ananikov VP (2016) Which metals are green for catalysis? Comparison of the toxicities of Ni, Cu, Fe, Pd, Pt, Rh, and Au salts. Angew Chem Int Ed 55:12150–12162
4. Mogren CL, Trumble JT (2010) The impacts of metals and metalloids on insect behaviour. Entomol Exp Appl 135:1–17
5. Karaoglu K, Yilmaz F, Menteşe E (2017) A new fluorescent "turn-off" Coumarin-based Chemosensor: synthesis, structure and cu-selective fluorescent sensing in water samples. J Fluoresc 27: 1293–1298
6. Chandra R, Ghorai A, Patra GK (2018) A simple benzildihydrazone derived colorimetric and fluorescent 'on-off-on' sensor for sequential detection of copper(II) and cyanide ions in aqueous solution. Sensors Actuators B Chem 255:701–711
7. Borase PN, Thale PB, Shankarling GS (2016) Dihydroquinazolinone based "turn-off" fluorescence sensor for detection of Cu^{2+} ions. Dyes Pigments 134:276–284
8. Ye F, Chai Q, Liang X-M, Li M-Q, Wang Z-Q, Fu Y (2017) A Highly Selective and Sensitive Fluorescent Turn-Off Probe for Cu^{2+} Based on a Guanidine Derivative. Molecules 22(10):1741
9. Shakir M, Abbasi A (2017) Solvent dependant isatin-based schiff base sensor as fluorescent switch for detection of Cu^{2+} and S^{2-} in human blood serum. Inorg Chim Acta 465:14–25
10. Saleh SM, Ali R, Ali IAI (2017) A novel, highly sensitive, selective, reversible and turn-on chemi-sensor based on Schiff base for rapid detection of Cu(II). Spectrochim Acta A Mol Biomol Spectrosc 183:225–231
11. Lee HG, Kim KB, Park GJ, Na Y, Jo HY, Lee SA, Kim C (2014) An anthracene-based fluorescent sensor for sequential detection of zinc and copper ions. Inorg Chem Commun 39:61–65
12. Malkondu S, Turhan D, Kocak A (2015) Copper(II)-directed static excimer formation of an anthracene-based highly selective fluorescent receptor. Tetrahedron Lett 56:162–167
13. Malkondu S, Turhan D, Kocak A (2015) A new turn-on fluorescent probe for the detection of copper ion in neat aqueous solution. Tetrahedron Lett 56:162–167
14. Su X, Aprahamian I (2014) Hydrazone-based switches, metallo-assemblies and sensors. Chem Soc Rev 43:1963–1981
15. Mukherjee S, Talukder S, Chowdhury S, Mal P, Evans HS (2016) Synthesis, structure and sensing behavior of hydrazone based chromogenic chemosensors for Cu^{2+} in aqueous environment. Inorg Chim Acta 450:216–224
16. Mukherjee S, Mal P, Evans HS (2014) Hydrazone based luminescent receptors for fluorescent sensing of Cu^{2+}: structure and spectroscopy. J Lumin 155:185–190
17. Mukherjee S, Mal P, Evans HS (2014) Complexation behavior of imidazoline hydrazones towards Cu^{2+} and Hg^{2+}: structure, sensing and DNA binding studies. Polyhedron 73:87–97
18. Mukherjee S, Mal P, Evans HS (2013) A new chromogenic and ratiometric agent for copper(II): synthesis, structure and spectroscopy. Polyhedron 50:495–501
19. Bhattacharyya A, Ghosh S, Makhal SC, Guchhait N (2018) Hydrazine appended self assembled benzoin-naphthalene conjugate as an efficient dual channel probe for Cu^{2+} and F^-: a spectroscopic investigation with live cell imaging for Cu^{2+} and practical performance for fluoride. J Photochem Photobiol A Chem 353: 488–498
20. Kim H, Rao BA, Jeong JW, Mallick S, Kang S-M, Choi JS, Lee C-S, Son Y-A (2015) A highly selective dual-channel $Cu^{2+}$and Al^{3+}chemodosimeter in aqueous systems: sensing in living cells and microfluidic flows. Sensors Actuators B Chem 210:173–182
21. Yun SH, Xia L, Edison TNJI, Pandurangan M, Kim DH, Kim SH, Lee YR (2017) Highly selective fluorescence turn-on sensor for Cu^{2+} ions and its application in confocal imaging of living cells. Sensors Actuators B Chem 240:988–995
22. Chang IJ, Choi MG, Jeong YA, Lee SH, Chang S-K (2017) Colorimetric determination of Cu^{2+} in simulated wastewater using naphthalimide-based Schiff base. Tetrahedron Lett 58:474–477
23. Ramdass A, Sathish V, Babu E, Velayudham M, Thanasekaran P, Rajagopal S (2017) Recent developments on optical and electrochemical sensing of copper(II) ion based on transition metal complexes. Coord Chem Rev 343:278–307
24. Yang L, Song Q, Og KD, Cao H (2013) Synthesis and spectral investigation of a turn-on fluorescence sensor with high affinity to Cu^{2+}. Sensors Actuators B Chem 176:181–185
25. Ge J-Z, Zou Y, Yan YH, Lin S, Zhao XF, Cao QY (2016) A new ferrocene–anthracene dyad for dual-signaling sensing of Cu(II) and Hg(II). J Photochem Photobiol B 315:67–75
26. Sivaraman G, Iniya M, Anand T, Kotla NG, Sunnapu O, Singaravadivel S, Gulyani A, Chellappa D (2018) Chemically diverse small molecule fluorescent chemosensors for copper ion. Coord Chem Rev 357:50–104
27. Liu S, Wang Y-M, Han J (2017) Fluorescent chemosensors for copper(II) ion: structure, mechanism and application. J Photochem Photobiol C 32:78–103
28. Kaur B, Kaur N, Kumar S (2018) Colorimetric metal ion sensors – a comprehensive review of the years 2011–2016. Coord Chem Rev 358:13–69
29. Aksamitowski P, Wieszczycka K, Wojciechowska I (2018) Selective copper extraction from sulfate media with N,N-dihexyl-N-hydroxypyridine-carboximidamides as extractants. Sep Purif Technol 201:186–192

30. Fu W, Chen Q, Hu H, Niu C, Zhu Q (2011) Solvent extraction of copper from ammoniacal chloride solutions by sterically hindered b-diketone extractants. Sep Purif Technol 80:52–58
31. Tanda BC, Oraby EA, Eksteen JJ (2017) Recovery of copper from alkaline glycine leach solution using solvent extraction. Sep Purif Technol 187:389–396
32. Xie F, Dreisinger DB (2010) Copper solvent extraction from alkaline cyanide solution with guanidine extractant LIX 7950. Trans Nonferrous Metal Soc China 20:1136–1140
33. Song J, Niu X, Li X-M, He T (2018) Selective separation of copper and nickel by membrane extraction using hydrophilic nanoporous ion-exchange barrier membranes. Process Saf Environ Prot 113:1–9
34. Wojciechowska I, Wieszczycka K, Aksamitowski P, Wojciechowska A (2017) A copper recovery from chloride solutions using liquid extraction with pyridinecarboximidamides as extractants. Sep Purif Technol 187:319–326
35. Yang R, Wang S, Duan H, Yuan X, Huang Z, Guo H, Yang X (2016) Efficient separation of copper and nickel from ammonium chloride solutions through the antagonistic effect of TRPO on Acorga M5640. Hydrometallurgy 163:18–23
36. Bidari E, Irannejad M, Gharabaghi M (2013) Solvent extraction recovery and separation of cadmium and copper from sulphate solution. J Environ Chem Eng 1:1269–1274
37. Rao KS, Devi NB, Reddy BR (2000) Solvent extraction of copper from sulphate medium using MOC 45 as extractant. Hydrometallurgy 57:269–275
38. Wieszczycka K, Tomczyk W (2011) Degradation of organothiophosphorous extractant Cyanex 301. J Hazard Mater 192:530–537
39. Liu D, Cao K, Jia Q (2013) Extraction of lead, copper, and bismuth with mixtures of N,N-di(1-methylheptyl) acetamide and neutral organophosphorus extractants. Sep Purif Technol 118:492–496
40. Jianga F, Yina S, Zhanga L, Penga J, Jua S, Millera JD, Wang X (2018) Solvent extraction of cu(II) from sulfate solutions containing Zn(II) and Fe (III) using an interdigital micromixer. Hydrometallurgy 177:116–122
41. Devi N (2016) Solvent extraction and separation of copper from base metals using bifunctional ionic liquid from sulfate medium. Trans Nonferrous Metals Soc China 26:874–881
42. Barache UB, Shaikh AB, Lokhande TN, Kamble GS, Anuse MA, Gaikwad SH (2018) An efficient, cost effective, sensing behaviour liquid-liquid extraction and spectrophotometric determination of copper(II) incorporated with 4-(4-chlorobenzylideneimino)-3-methyl-5-mercapto-1, 2, 4-triazole: analysis of food samples, leafy vegetables, fertilizers and environmental samples. Spectrochim Acta A Mol Biomol Spectrosc 189:443–453
43. Wasylka JP, Owczarek K, Namieśnik J (2016) Modern solutions in the field of microextraction using liquid as a medium of extraction. Trends Anal Chem 85:46–64
44. Sahin CA, Tokgoz I (2010) A novel solidified floating organic drop microextraction method for preconcentration and determination of copper ions by flow injection flame atomic absorption spectrometry. Anal Chim Acta 667:83–87
45. Sharifi V, Abbasi A, Nosrati A (2016) Application of hollow fiber liquid phase microextraction and dispersive liquid liquid microextraction techniques in analytical toxicology. J Food Drug Anal 24:264–276
46. Yazdi AS, Amiri A (2010) Liquid-phase microextraction. Trends Anal Chem 29:1
47. Bauer C, Bauduin P, Dufrˆeche JF, Zemb T, Diat O (2012) Liquid/liquid metal extraction: phase diagram topology resulting from molecular interactions between extractant, ion, oil and water. Eur Phys J Special Topics 213:225–241
48. Jeannot MA, Przyjazny A, Kokosa JM (2010) Single drop microextraction—development, applications and future trends. J Chromatogr A 1217(16):2326–2336
49. Miller MT, Gantzel PK, Karpishin TB (1999) Effects of Sterics and electronic delocalization on the Photophysical, structural, and electrochemical properties of 2,9-Disubstituted 1,10-Phenanthroline copper(I) complexes. Inorg Chem 38:3414–3422
50. Zoubi WA, Kandil F, Chebani MK (2016) Solvent extraction of chromium and copper using Schiff base derived from terephthaldialdehyde and 5-amino-2-methoxy-phenol. Arab J Chem 9:526–531
51. Yamina B (2016) Extractive separation of Cu^{2+}–Co^{2+} and Ni^{2+}–Co^{2+} mixtures using N-Salicylideneaniline. Russ J Phys Chem A 90(13):2642–2645
52. Parhi PK, Park KH, Nam CW, Park JT (2015) Liquid-liquid extraction and separation of total rare earth (RE) metals from polymetallic manganese nodule leaching solution. J Rare Earths 33(2):207–213
53. Sinha MK, Sahu SK, Meshram P, Pandey BD, Kumar V (2012) Solvent extraction and separation of copper and zinc from a pickling solution. Int J Metall Mater Eng 1(2):28–34
54. Mehlig JP (1941) Colorimetric determination of copper with ammonia a spectrophotometric study. Anal Chem 13(8):533–535
55. Luo Y, Xu Y, Zhi C, A Color Channel Ratio Image based object detection method in complex scenario, ISBN: 978-1-4673-6047-0, https://doi.org/10.1109/BMSB.2013.6621737